

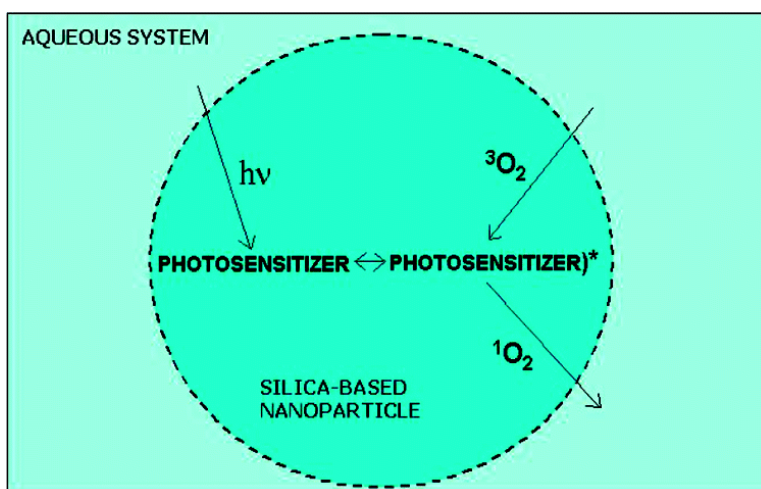
Article

Ceramic-Based Nanoparticles Entrapping Water-Insoluble Photosensitizing Anticancer Drugs: A Novel Drug–Carrier System for Photodynamic Therapy

Indrajit Roy, Tymish Y. Ohulchanskyy, Haridas E. Pudavar, Earl J. Bergey, Allan R. Oseroff, Janet Morgan, Thomas J. Dougherty, and Paras N. Prasad

J. Am. Chem. Soc., **2003**, 125 (26), 7860-7865 • DOI: 10.1021/ja0343095 • Publication Date (Web): 10 June 2003

Downloaded from <http://pubs.acs.org> on March 29, 2009



More About This Article

Additional resources and features associated with this article are available within the HTML version:

- Supporting Information
- Links to the 48 articles that cite this article, as of the time of this article download
- Access to high resolution figures
- Links to articles and content related to this article
- Copyright permission to reproduce figures and/or text from this article

[View the Full Text HTML](#)



ACS Publications
 High quality. High impact.

Ceramic-Based Nanoparticles Entrapping Water-Insoluble Photosensitizing Anticancer Drugs: A Novel Drug–Carrier System for Photodynamic Therapy

Indrajit Roy,[†] Tymish Y. Ohulchanskyy,[†] Haridas E. Pudavar,[†] Earl J. Bergey,[†] Allan R. Oseroff,^{†,‡} Janet Morgan,[‡] Thomas J. Dougherty,[§] and Paras N. Prasad^{*,†}

Contribution from the Institute of Lasers, Photonics and Biophotonics, Department of Chemistry, State University of New York, Buffalo, New York 14260-3000, and Department of Dermatology and Photodynamic Therapy Center, Roswell Park Cancer Institute, Buffalo, New York 14263

Received January 23, 2003; E-mail: pnprasad@buffalo.edu

Abstract: A novel nanoparticle-based drug carrier for photodynamic therapy is reported which can provide stable aqueous dispersion of hydrophobic photosensitizers, yet preserve the key step of photogeneration of singlet oxygen, necessary for photodynamic action. A multidisciplinary approach is utilized which involves (i) nanochemistry in micellar cavity to produce these carriers, (ii) spectroscopy to confirm singlet oxygen production, and (iii) in vitro studies using tumor cells to investigate drug–carrier uptake and destruction of cancer cells by photodynamic action. Ultrafine organically modified silica-based nanoparticles (diameter ~30 nm), entrapping water-insoluble photosensitizing anticancer drug 2-devinyl-2-(1-hexyloxyethyl) pyropheophorbide, have been synthesized in the nonpolar core of micelles by hydrolysis of triethoxyvinylsilane. The resulting drug-doped nanoparticles are spherical, highly monodispersed, and stable in aqueous system. The entrapped drug is more fluorescent in aqueous medium than the free drug, permitting use of fluorescence bioimaging studies. Irradiation of the photosensitizing drug entrapped in nanoparticles with light of suitable wavelength results in efficient generation of singlet oxygen, which is made possible by the inherent porosity of the nanoparticles. In vitro studies have demonstrated the active uptake of drug-doped nanoparticles into the cytosol of tumor cells. Significant damage to such impregnated tumor cells was observed upon irradiation with light of wavelength 650 nm. Thus, the potential of using ceramic-based nanoparticles as drug carriers for photodynamic therapy has been demonstrated.

Introduction

Photodynamic therapy is an emerging modality for the treatment of a variety of oncological, cardiovascular, dermatological, and ophthalmic diseases.^{1,3} Photodynamic therapy is based on the concept that light-sensitive species or photosensitizers (PSs) can be preferentially localized in tumor tissues upon systemic administration.^{3,4} When such photosensitizers are irradiated with an appropriate wavelength of visible or near-infrared (NIR) light, the excited molecules can transfer their energy to molecular oxygen in the surroundings, which is normally in its triplet ground state. This results in the formation of reactive oxygen species (ROSs), such as singlet oxygen (¹O₂) or free radicals. ROSs are responsible for oxidizing various cellular compartments including plasma, mitochondria, lysosomal, and nuclear membranes, etc., resulting in irreversible

damage of tumor cells.^{1–5} Therefore, under appropriate conditions, photodynamic therapy offers the advantage of an effective and selective method of destroying diseased tissues without damaging adjacent healthy ones.^{1,4}

However, most photosensitizing drugs (PSs) are hydrophobic, i.e., poorly water soluble, and therefore, preparation of pharmaceutical formulations for parenteral administration is highly hampered.^{3,6} To overcome this difficulty, different strategies have evolved to enable a stable dispersion of these drugs into aqueous systems, often by means of a delivery vehicle. Upon systemic administration, such drug-doped carriers are preferentially taken up by tumor tissues by virtue of the “enhanced permeability and retention effect”,^{3,7} which is the property of such tissues to engulf and retain circulating macromolecules and particles owing to their “leaky” vasculature. The carriers include oil dispersions (micelles), liposomes, low-density lipoproteins, polymeric micelles, and hydrophilic drug–polymer complexes. Oil-based drug formulations (micellar systems) using nonionic polyoxyethylated castor oils (e.g., Tween-80, Cremophor-EL, or CRM, etc.) have shown enhanced drug loading and

* To whom correspondence should be addressed.

[†] State University of New York.

[‡] Department of Dermatology, Roswell Park Cancer Institute.

[§] Photodynamic Therapy Center, Roswell Park Cancer Institute.

(1) Prasad, P. N. *Introduction to Biophotonics*; John Wiley & Sons: New York, 2003.

(2) Levy, J. G.; Obochi, M. *Photochem. Photobiol.* **1996**, *64*, 737–739.

(3) Konan, Y. N.; Gruny, R.; Allemann, E. *J. Photochem. Photobiol., B* **2002**, *66*, 89–106.

(4) Hasan, T.; Moor, A. C. E.; Ortel, B. *Cancer Medicine*, 5th ed.; B.C. Decker, Inc.: Hamilton, Ontario, Canada, 2000.

(5) Dougherty, T. J. *Photochem. Photobiol.* **1987**, *45*, 879–889.

(6) Taillefer, J.; Jones, M. C.; Brasseur, N.; Van Lier, J. E.; Leroux, J. C. *J. Pharm. Sci.* **2000**, *89*, 52–62.

(7) Duncan, R. *Pharm. Sci. Technol. Today* **1999**, *2*, 441–449.

improved tumor uptake over free drugs, presumably due to interaction with plasma lipoproteins in blood.^{8,9} However, such emulsifying agents also have been reported to elicit acute hypersensitivity (anaphylactic) reactions in vivo.^{10,11} Liposomes are concentric phospholipid bilayers encapsulating aqueous compartments, which can contain hydrophilic and lipophilic drugs.³ Although the tumor uptake of the liposomal formulation of drugs is better than that of simple aqueous dispersions, many suffer from poor drug loading and increased self-aggregation of the drug in the entrapped state.^{3,12,13} Liposomes are also prone to opsonization and subsequent capture by the major defense system of the body (reticuloendothelial system, or RES).¹³ Recently, drugs incorporated inside pH-sensitive polymeric micelles have shown improved tumor phototoxicity compared to Cremophor-EL formulations in vitro. However, in vivo studies resulted in poor tumor regression and increased accumulation in normal tissues.^{6,14} Another major disadvantage, common to all the above-mentioned delivery systems, which are based on controlled release of the photosensitive drugs, is the posttreatment accumulation of the free drugs in the skin and the eye, resulting in phototoxic side effects, which may last for at least a month.¹⁵

Hydrated ceramic-based nanoparticles, doped with photosensitive drugs, carry the promise of solving many of the problems associated with free as well as polymer-encapsulated drugs. Such ceramic particles have a number of advantages over organic polymeric particles. First, the preparative processes involved, which are quite similar to the well-known sol-gel process,^{16,17} require simple, ambient temperature conditions. These particles can be prepared with the desired size, shape, and porosity, and are extremely stable. Their ultralow size (less than 50 nm) can help them evade capture by the RES. In addition, there are no swelling or porosity changes with a change in pH, and they are not vulnerable to microbial attack.¹⁸ These particles also effectively protect doped molecules (enzymes, drugs, etc.) against denaturation induced by extreme pH and temperature.¹⁹ Such particles, including silica, alumina, titania, etc., are also known for their compatibility in biological systems.^{19–21} In addition, their surfaces can be easily modified with different functional groups.^{21,22} Therefore, they can be attached to a variety of monoclonal antibodies or other ligands to target them to desired sites in vivo.

The synthesis of ceramic nanoparticles, mostly but not exclusively based on silica, has been extensively reported in the literature,^{23,24} although their application in drug delivery has not yet been fully exploited. Ceramic nanoparticles are highly stable, and may not release any encapsulated biomolecules even at extreme conditions of pH and temperature.¹⁹ Conventional drug delivery methods require the carrier vehicle to free the encapsulated drug to elicit the appropriate biological response.⁴ However, this is not a prerequisite when macromolecular carrier molecules are used for the delivery of photosensitizing drugs in photodynamic therapy.^{4,25} Keeping this in mind, we have developed ceramic-based nanoparticles as carriers of photosensitizing drugs for applications in photodynamic therapy. Although these particles do not release the entrapped drugs, their porous matrix is permeable to molecular as well as singlet oxygen. Therefore, the desired photodestructive effect of the drug will be maintained even in the encapsulated form.

In this paper, we report the synthesis of photosensitizer-doped organically modified silica-based nanoparticles (diameter ~30 nm), by controlled hydrolysis of triethoxyvinylsilane in micellar media. The drug/dye used is 2-devinyl-2-(1-hexyloxyethyl) pyropheophorbide (HPPH), an effective photosensitizer which is in phase I/II clinical trials at the Roswell Park Cancer Institute, Buffalo, NY.²⁶ The synthesized doped particles were shown to be spherical and highly monodispersed. The loss of fluorescence of the entrapped photosensitizing drug is largely prevented in aqueous media in contrast to that of the free one. Upon light irradiation, the entrapped drug is able to efficiently generate singlet oxygen. The doped nanoparticles are actively taken up by tumor cells, and irradiation with visible light has resulted in irreversible destruction of such impregnated cells. These observations suggest the potential of ceramic-based particles as carriers for photodynamic drugs.

Experimental Section

Materials. Surfactant Aerosol OT (AOT; 98%), cosurfactant 1-butanol (99.8%), triethoxyvinylsilane (TEVS; 97%), and 3-aminopropyltriethoxysilane (APTES; 99%) were purchased from Aldrich. MTT [3-(4,5-dimethylthiazol-2-yl)-2,5-diphenyltetrazolium bromide] and 2-propanol are products of Sigma. *N,N*-Dimethylformamide (DMF) was purchased from Fisher Chemicals. Deuterium oxide (99.9 atom % D) was obtained from Isotec Inc. The drug HPPH was provided by the Roswell Park Cancer Institute. The dye anthracenedipropionic acid disodium salt was purchased from Molecular Probes. Cell culture products, unless mentioned otherwise, were purchased from GIBCO. All the above chemicals were used without any further purification.

Synthesis and Characterization of Drug-Loaded Silica-Based Nanoparticles. The nanoparticles, both void and drug-loaded, were synthesized in the nonpolar core of AOT/1-butanol/water micelles, as shown schematically in Figure 1. In a typical experiment, the micelles were prepared by dissolving 0.44 g of AOT and 800 μ L (0.56 g) of 1-butanol in 20 mL of doubly distilled water by vigorous magnetic stirring. A 30 μ L sample of HPPH in DMF (15 mM) was dissolved by magnetic stirring in the resulting clear solution. For void nanoparticles, 30 μ L of DMF without HPPH was added. Neat triethoxyvinylsilane (200 μ L) was added to the micellar system, and the resulting solution was stirred for about 1 h, or until it became clear. After that, 10 μ L of

- (8) Kongshaug, M.; Moan, J.; Cheng, L. S.; Garbo, G. M.; Kolboe, S.; Morgan, A. R.; Rimington, C. *Int. J. Biochem.* **1993**, *25*, 739–760.
- (9) Woodburn, K.; Kessel, D. *J. Photochem. Photobiol., B* **1994**, *22*, 197–201.
- (10) Dye, D.; Watkins, J. *Br. Med. J.* **1980**, *280*, 1353–1353.
- (11) Michaud, L. B. *Ann. Pharmacother.* **1997**, *31*, 1402–1404.
- (12) Damoiseau, X.; Schuitemaker, H. J.; Lagerberg, J. W. M.; Hoebeke, M. *J. Photochem. Photobiol., B* **2001**, *60*, 50–60.
- (13) Isele, U.; Schieweck, K.; Kessler, R.; Hoogevest, P. V.; Caparo, H. G. *J. Pharm. Sci.* **1995**, *84*, 166–173.
- (14) Taillefer, J.; Brasseur, N.; Van Lier, J. E.; Lenearts, V.; Le Garrec, D.; Leroux, J. C. *J. Pharm. Pharmacol.* **2001**, *53*, 155–166.
- (15) Dillon, J.; Kennedy, J. C.; Pottier, R. H.; Roberts, J. E. *Photochem. Photobiol.* **1988**, *48*, 235–238.
- (16) Brinker, C. J.; Schrer, G. *Sol-Gel Science: The Physics and Chemistry of Sol-Gel Processing*; Academic Press: San Diego, 1990.
- (17) Avnir, D.; Braun, S.; Lev, O.; Ottolenghi, O. *Chem. Mater.* **1994**, *6*, 1605–1614.
- (18) Weetal, H. H. *Biochim. Biophys. Acta* **1970**, *212*, 1–7.
- (19) Jain, T. K.; Roy, I.; De, T. K.; Maitra, A. N. *J. Am. Chem. Soc.* **1998**, *120*, 11092–11095.
- (20) Shimada, M.; Shoji, N.; Takahashi, A. *Anticancer Res.* **1995**, *15*, 109–115.
- (21) Lal, M.; Levy, L.; Kim, K. S.; He, G. S.; Wang, X.; Min, Y. H.; Pakatchi, S.; Prasad, P. N. *Chem. Mater.* **2000**, *12*, 2632–2639.
- (22) Badley, R. D.; Warren, T. F.; McEnroe, F. J.; Assink, R. A. *Langmuir* **1990**, *6*, 792–801.

- (23) Arriagada, F. J.; Osseo-Asare, K. *J. Colloid Interface Sci.* **1995**, *170*, 8–17.
- (24) Chang, C.; Fogler, H. S. *AIChE J.* **1996**, *42*, 3153–3163.
- (25) Hasan, T. *Photodynamic therapy: basic principles and clinical applications*; Marcel Dekker: New York, 1992.
- (26) Henderson, B. W.; Bellnier, D. A.; Graco, W. R.; Sharma, A.; Pandey, R. K.; Vaughan, L.; Weishaupt, K.; Dougherty, T. J. *Cancer Res.* **1997**, *57*, 4000–4007.

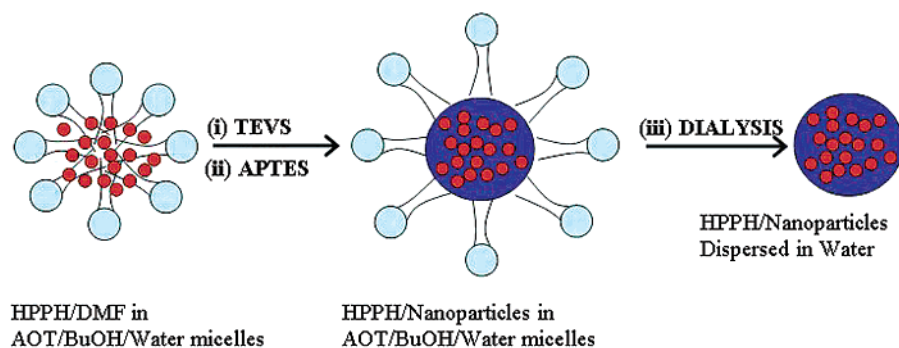


Figure 1. Scheme depicting the synthesis and purification of HPPH-doped silica-based nanoparticles in a micellar medium.

neat 3-aminopropyltriethoxysilane was added and the system stirred for about 20 h. The entire reaction was carried out at room temperature. At the end of the process, a blue-white translucency indicating the formation of nanoparticles was observed. After the formation of drug-doped nanoparticles, surfactant AOT and cosurfactant 1-butanol were completely removed by dialyzing the solution against water in a 12–14 kDa cutoff cellulose membrane (Spectrum Laboratories, Inc.) for 48 h. The dialyzed solution was then filtered through a 0.2 μm cutoff membrane filter (Nalgene) and used for further experimentation.

Transmission electron microscopy (TEM) was employed to determine the morphology and size of the aqueous dispersion of nanoparticles, using a JEOL JEM 2020 electron microscope, operating at an accelerating voltage of 200 kV. UV–vis absorption spectra were recorded using a Shimadzu UV-3101 PC spectrophotometer, in a quartz cuvette with 1 cm path length. Fluorescence spectra were recorded on a Shimadzu RF 5000U spectrofluorimeter.

Detection of Singlet Oxygen by the Luminescence Spectroscopy Method. Detection of singlet oxygen ($^1\text{O}_2$) has been extensively reported by its luminescence emission spectra at 1270 nm.^{27,28} We have used deuterium oxide (D_2O) as a solvent because it extends the lifetime of singlet oxygen compared to water. In a typical experiment, 3 mL of 22.5 μM HPPH entrapped in nanoparticles and dispersed in D_2O was used. HPPH solubilized in AOT/BuOH/ D_2O micelles and void nanoparticles in D_2O were used as positive and negative controls, respectively. A SPEX 270M spectrometer (Jobin Yvon) equipped with an InGaAs photodetector (Electro-Optical Systems Inc.) was used for recording singlet oxygen emission spectra. A diode-pumped solid-state laser (Verdi, Coherent) at 532 nm was the excitation source. The sample solution in a quartz cuvette was placed directly in front of the entrance slit of the spectrometer, and the emission signal was collected at 90° relative to the exciting laser beam. An additional long-pass filter (850LP) was used to attenuate the excitation laser and the fluorescence from HPPH.

Singlet Oxygen Detection by a Chemical Method. In addition to the luminescence spectroscopy method, generation of singlet oxygen was also detected chemically, using the disodium salt of 9,10-anthracenedipropionic acid as a singlet oxygen sensor.²⁹ Disodium 9,10-anthracenedipropionic acid (a water-soluble anthracene derivative) is bleached by singlet oxygen to its corresponding endoperoxide. The reaction was monitored spectrophotometrically by recording the decrease in optical density at 400 nm (λ_{max} of ADPA). In a typical experiment, 150 μL of disodium 9,10-anthracenedipropionic acid in D_2O (5.5 mM) was mixed with 3 mL of 15 μM HPPH (in AOT/ D_2O micelles or entrapped in nanoparticles in D_2O). The control experiment used disodium 9,10-anthracenedipropionic acid mixed with void nanoparticles dispersed in D_2O . The solutions were irradiated with a

650 nm laser source (solid-state diode-pumped laser), and their optical densities at 400 nm were recorded every 10 min in a spectrophotometer.

In Vitro Studies with Tumor Cells: Nanoparticle Uptake, Imaging, and Viability Assay. Using established cell cultures, the following protocol was followed for each cell line used. For this experiment, two cell lines were used: UCI-107 (University of California, Irvine, CA) and HeLa (ATCC, Manassas, VA), both maintained in MEM α medium with 5% and 10% fetal bovine serum (FBS), respectively.

For studying nanoparticle uptake and imaging, the cells were trypsinized and resuspended in medium at a concentration of 7.5×10^5 cells/mL. Then on 60 mm culture plates, 5 mL of medium was combined with 0.10 mL of cell suspension. The plates were then placed overnight in an incubator at 37 °C with 5% CO_2 (VWR Scientific model 2400, Bridgeport, NJ). The next day, the cells (with about 50% confluence) were carefully rinsed with phosphate-buffered saline (PBS), and 5 mL of medium was replaced on the plates. At this stage, 500 μL of an aqueous dispersion of HPPH-doped nanoparticles (22 μM) was added to each plate and mixed gently. The final concentration of HPPH on each plate was 2 μM . The treated cells were returned to the incubator (37 °C, 5% CO_2) for an hour. After incubation, the plates were rinsed with sterile PBS, and fresh medium was replaced at a volume of 5 mL/plate. The cells were then directly imaged under a confocal laser scanning microscope (MRC-1024, Bio-Rad, Richmond, CA), which was attached to an upright microscope (Nikon model Eclipse E800). A water immersion objective lens (Nikon, Fluor-60X, NA = 1.0) was used for cell imaging. A solid-state diode-pumped laser (Verdi, Coherent) was used as a source of excitation (532 nm). A long-pass filter (585 LP, 585 nm) and an additional filter with transmission at 680 ± 15 nm (Chroma 680/30) were used as emission filters for imaging. To check whether an observed fluorescence is from entrapped HPPH, we used localized spectrofluorometry on the cells.³⁰ The fluorescence signal was collected without filtering from the upper port of the confocal microscope using a multimode optical fiber of core diameter 1 mm, and was delivered to a spectrometer (Holospec from Kaiser Optical Systems, Inc.) equipped with a cooled charge coupled device (CCD) camera (Princeton Instruments) as a detector. A comparison of the fluorescence spectra of the cells and the fluorescence spectra of HPPH allows us to confirm the origin of fluorescence as seen in the fluorescence image channel.

For studying cell viability, 24-well plates were inoculated with cells (7.5×10^5 cells/well) overnight. The medium was removed, the wells were rinsed carefully three times using sterile PBS, and 2 mL of fresh medium was replaced into each well. Predetermined concentrations of the drug, as confirmed by absorption measurements, on (a) 20 μM HPPH in 120 μL of 0.25% Tween-80/water micelles, (b) 20 μM HPPH encapsulated in 120 μL of aqueous nanoparticle dispersion, (c) 120 μL of 0.25% Tween-80/water micelles, and (d) 120 μL of aqueous

(27) Frederiksen, P. K.; Jorgensen, M.; Ogilby, P. R. *J. Am. Chem. Soc.* **2001**, *123*, 1215–1221.
 (28) Karotki, A.; Kruk, M.; Drobizhev, M.; Rebane, A.; Nickel, E.; Spangler, C. W. *IEEE J. Quantum Electron.* **2001**, *7*, 971–975.
 (29) Lindig, B. A.; Rodgers, M. A. J.; Schaap, A. P. *J. Am. Chem. Soc.* **1980**, *102*, 5590–5593.

(30) Wang, X.; Pudavar, H. E.; Kapoor, R.; Krebs, L. J.; Bergey, E. J.; Liebow, C.; Prasad, P. N.; Nagy, A.; Schally, A. V. *J. Biomed. Opt.* **2001**, *6*, 319–325.

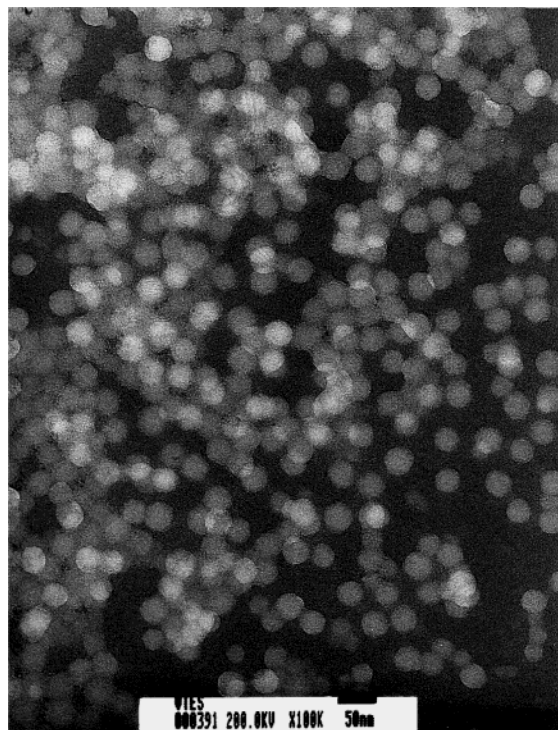


Figure 2. TEM picture of HPPH-doped silica-based nanoparticles showing highly monodispersed particles with an average diameter of 30 nm.

void nanoparticle dispersion were added to designated wells at this time. The plates were then returned to the incubator for 2 h. Next, the wells were rinsed three times with sterile PBS. A 2 mL sample of fresh medium was added, and the wells were immediately exposed to a 650 nm laser light source for 10 min each. The power at the cell level was ~ 1.4 mW/cm². The plates were returned to the incubator overnight. Cell viability was estimated by means of the colorimetric MTT assay.³¹ In the MTT assay, the absorbance of formazan (produced by the cleavage of MTT by dehydrogenases in living cells) at 570 nm is directly proportional to the number of live cells.³¹ Briefly, MTT was dissolved in sterile PBS at 5 mg/mL, and 200 μ L was added to each well. The plate was then incubated at 37 °C with 5% CO₂ for 4 h. After incubation, the medium was carefully aspirated, and any purple MTT formazan crystals were dissolved in 2 mL of 0.1 N HCl in anhydrous 2-propanol. The absorbance was measured at 570 nm using a Bausch & Lomb Spectronic 601 spectrophotometer. Cells incubated with serum-supplemented medium only represent 100% cell survival. 4-fold replicates were run per drug and light dose, and each experiment was repeated three times.

All the experiments were carried out under room temperature, unless otherwise mentioned.

Results and Discussions

A TEM image of the drug-loaded nanoparticles is shown in Figure 2. The particles are spherical, having uniform size distribution, with an average size of 30 nm.

The absorption spectra of HPPH, in AOT/BuOH/water micelles and entrapped in nanoparticles, are similar (Figure 3), indicating no changes in the HPPH chromophore upon entrapment inside nanoparticles. Nanoparticles without HPPH show virtually no absorption in the range of 600–900 nm. This region is considered to be the useful therapeutic region in photodynamic therapy due to the high tissue penetration of light at these wavelengths.⁴ Such particles can therefore be used as drug carriers in photodynamic therapy, since they do not affect the

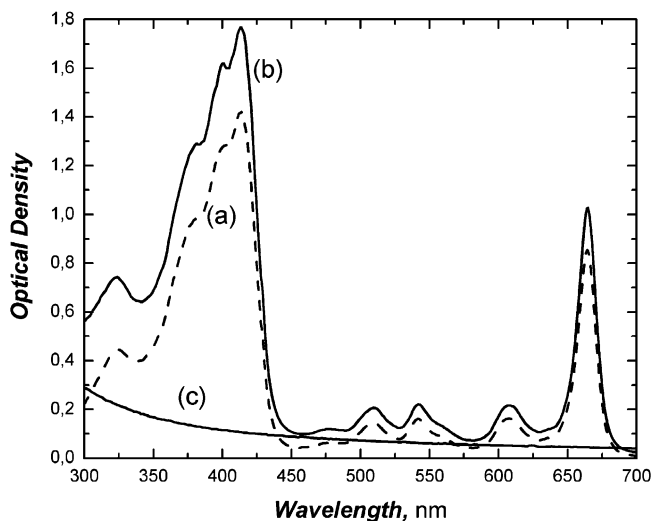


Figure 3. Absorption spectra of (a) HPPH in AOT/BuOH/water micelles, (b) HPPH-doped silica nanoparticles, and (c) void silica nanoparticles.

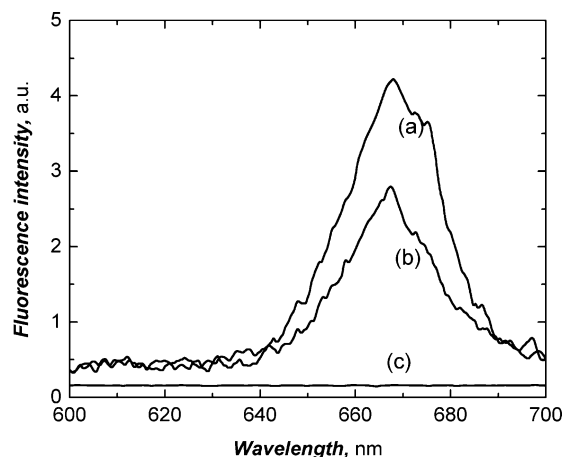


Figure 4. Fluorescence emission spectra of (a) HPPH-doped silica nanoparticles before dialysis, (b) HPPH-doped silica nanoparticles after dialysis, and (c) HPPH dissolved in 0.2% DMF/water. The excitation wavelength is 414 nm.

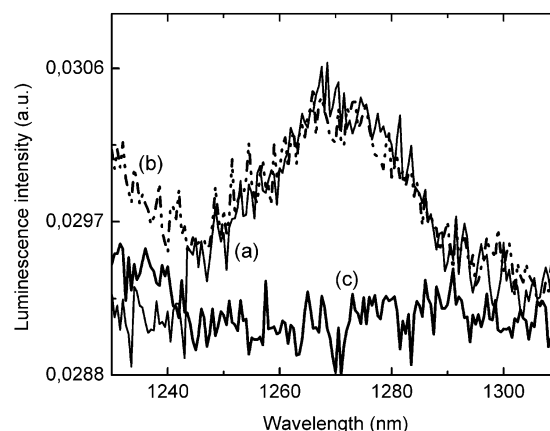


Figure 5. Luminescence emission spectra of generated singlet oxygen at 1270 nm of (a) HPPH in AOT/BuOH/D₂O micelles (solid line), (b) HPPH-doped silica nanoparticles dispersed in D₂O, and (c) void silica nanoparticles in D₂O.

absorbance of the entrapped drug and are inert to the therapeutic light used.

Figure 4 represents the fluorescence emission spectra of aqueous dispersion of HPPH entrapped in nanoparticles. The

(31) Mosmann, T. *J. Immunol. Methods* **1983**, *65*, 55–63.

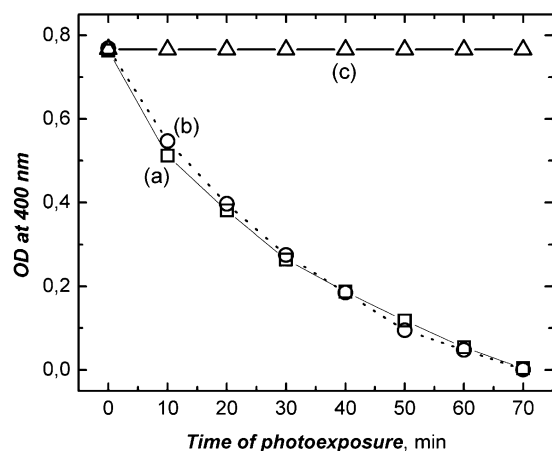


Figure 6. Time-dependent bleaching of disodium 9,10-anthracenedipropionic acid caused by singlet oxygen generated by (a) HPPH in AOT/BuOH/D₂O micelles, (b) HPPH-doped silica nanoparticles dispersed in D₂O, and (c) void silica nanoparticles in D₂O. The change in disodium 9,10-anthracenedipropionic acid absorption at 400 nm upon photoirradiation was monitored as a function of time.

spectra were recorded both before and after dialysis against distilled water (which effectively eliminates the surfactant and cosurfactant molecules used). After dialysis, the emission signal from the HPPH in the nanoparticles is almost 70% that obtained before dialysis. In contrast, the same concentration of free HPPH in 0.2% DMF/water (20 μ L of a 15 mM HPPH/DMF solution was dispersed in 10 mL of water) exhibited practically no emission, though it showed absorption similar to that of HPPH in nanoparticles. This absence of fluorescence of the nonpolar drug dispersed in a polar solvent can be due to either drug–solvent interaction promoting nonradiative decay or concentration quenching derived from self-aggregation of nonpolar drugs. But in the case of HPPH/nanoparticles, the drug molecules can be envisaged as discretely embedded in the particle matrix (Figure 1), and therefore protected from exposure to the aqueous environment, preventing a complete loss of fluorescence. The property of resistance to fluorescence quenching in aqueous media by entrapped nonpolar drugs/dyes can be exploited to fabricate nanoprobe for imaging in biological systems.

We now hypothesize that, since ceramic matrixes are generally porous, photosensitizing drugs entrapped within them can interact with molecular oxygen which has diffused through the pores. This can lead to the formation of singlet oxygen by energy transfer from the excited photosensitizer to molecular oxygen, which can then diffuse out of the porous matrix to produce a cytotoxic effect in tumor cells. To test this hypothesis, we studied the generation of singlet oxygen, after excitation of HPPH, by its luminescence emission spectra at 1270 nm. Figure 5 shows the spectra for HPPH, solubilized in micelles as well as entrapped in nanoparticles. Both spectra show similar intensities and peak positions (1270 nm), indicating similar efficiencies of singlet oxygen generation in both cases. It should be noted that the absorption spectra of HPPH were also similar for the two. A control spectrum, using nanoparticles without HPPH, shows no singlet oxygen luminescence.

We confirmed singlet oxygen generation by a chemical method as described in the Experimental Section,²⁹ using the disodium salt of 9,10-anthracenedipropionic acid as a detector. Figure 6 shows the decrease in optical density (OD) at 400 nm (absorption maximum for disodium 9,10-anthracenedipropionic acid), in different samples (aqueous dispersions of HPPH/micelles, HPPH/nanoparticles, and nanoparticles without HPPH), as a function of the time of light exposure. The plots for HPPH, solubilized in micelles or doped in nanoparticles, show a sharp decrease in OD with the time of light exposure, indicating the generation of singlet oxygen with similar efficiencies in both cases. The nanoparticles without HPPH produced no change in the OD of disodium 9,10-anthracenedipropionic acid with time, confirming that the bleaching of disodium 9,10-anthracenedipropionic acid in the presence of HPPH is caused by the generated singlet oxygen and not by the irradiating light.

Fluorescence imaging was used to determine whether HPPH/nanoparticles were taken up by tumor cells. The fluorescence images of HeLa (Figure 7A) and UCI-107 (Figure 7B) cells show significant intracellular staining in the cytoplasm, indicating accumulation of nanoparticles. Localized spectra of the cytoplasm, shown in Figure 7 (insets), show the characteristic fluorescence emission peak for HPPH (~665 nm), indicating

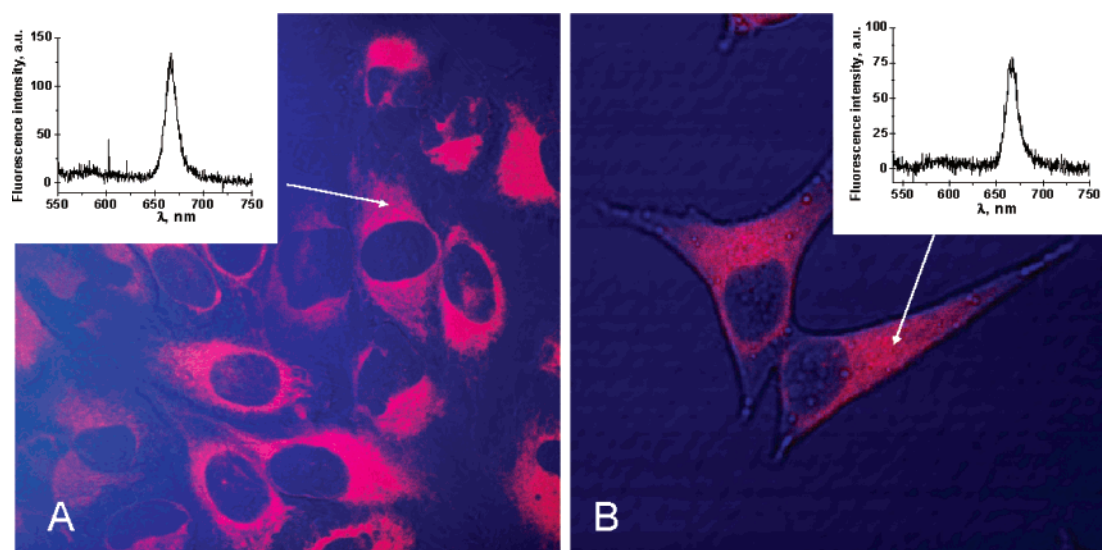


Figure 7. Confocal fluorescence image of tumor cells (A) HeLa and (B) UCI-107 treated with HPPH-doped nanoparticles. Transmission (blue) and fluorescence (red) channels are shown. (Inset) Localized fluorescence spectra from the cytoplasm of the treated cell. Excitation is at 532 nm.

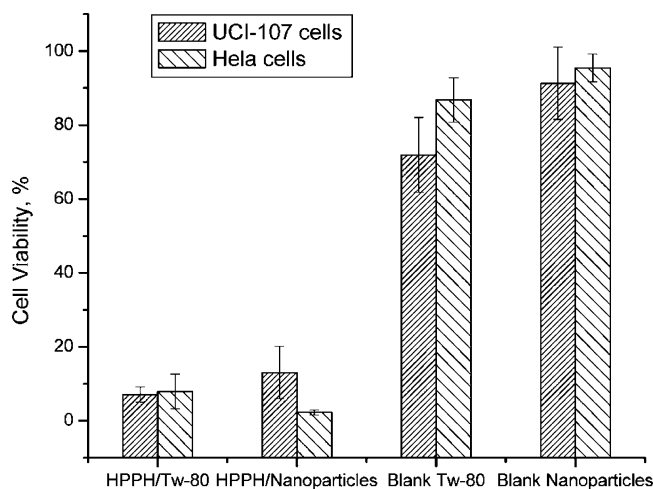


Figure 8. Percentage of cell survival of UCI-107 and HeLa cells, after treatment with various samples and subsequent irradiation with 650 nm laser light (with reference to irradiated but untreated cells as having 100% survival). Cell viability was assayed by the MTT method (values: mean \pm standard deviation).

that the signal is not due to autofluorescence. The cells were viable (verified morphologically) in the dark even after 10 h of staining, indicating low dark toxicity from the particles.

The cell phototoxicity study, represented in Figure 8, shows the percentage of cell survival after treatment of UCI-107 and HeLa tumor cells with various agents (cells without treatment were used as a control) and subsequent photoactivation using a 650 nm laser. Significant cell death can be observed for both HPPH/Tween-80 micelles and HPPH/nanoparticles. In addition, some cellular toxicity can be observed for blank Tween-80 micelles, which is supposed to be a nontoxic surfactant. In comparison blank nanoparticles exhibit much less toxicity. The data show that HPPH-doped nanoparticles are an effective drug-carrier system for killing tumor cells in vitro by light exposure. Experiments using this drug-carrier system on tumor-model animals are in progress.

Conclusions

Ultrafine organically modified silica-based nanoparticles, doped with a water-insoluble photosensitizing anticancer drug, HPPH, have been synthesized. The doped particles are uniform in size distribution with an average diameter of 30 nm, and can

be formulated as a stable aqueous dispersion. Although the drug is embedded inside the particle matrix, it can be excited by irradiation with light of appropriate wavelength, to generate singlet oxygen, which can effect photodynamic therapy. Such doped nanoparticles are efficiently taken up by tumor cells in vitro, and light irradiation of such impregnated cells results in significant cell death. These observations have illustrated the potential of ceramic-based matrixes as drug carriers for photodynamic therapy. Their extreme stability compared with polymeric carrier systems,¹⁹ together with their biocompatibility,^{19–21} and ease of surface modification,^{22,23} suggests enormous potential for developing injectable formulations of drug-loaded ceramic vehicles for safe and efficient trafficking to tumor tissues in vivo. Recently, our group has reported the synthesis of silica-based nanoparticles which encapsulate a magnetic core.³² These particles were functionalized with a peptide hormone-targeting agent, leutinizing hormone releasing hormone (LH-RH). The resulting “nanoclinic” was shown to selectively target LH-RH receptor-positive tumor cells. Exposure to a dc magnetic field then resulted in the selective magnetocytotoxicity of the receptor-positive cells only.³³ At present, we are working on functionalizing the silica surface with different ligands to target our particles to tumor cells containing such ligand-specific receptors. Work also is under way involving the synthesis of functionalized magnetic nanoparticles (similar to the nanoclinic described above) as carriers of photosensitive drugs to develop a drug-carrier system with “dual lethality”, combining the photocytotoxic effect of the drug with the magnetocytotoxic property of the carrier vehicle itself.

Acknowledgment. This study was supported by the Directorate of Chemistry and Life Sciences of the Air Force Office of Scientific Research through Defense University Research Initiative on Nanotechnology (DURINT) Grant No. F496200110358 and Grant No. CA5579 from the National Institutes of Health. We also thank Lisa A. Vathy for her excellent technical support.

JA0343095

- (32) Levy, L.; Sahoo, Y.; Kim, K. S.; Bergey, E. J.; Prasad, P. N. *Chem. Mater.* **2002**, *14*, 3715–3721.
 (33) Bergey, E. J.; Levy, L.; Wang, X.; Krebs, L. J.; Lal, M.; Kim, K. S.; Pakatchi, S.; Liebow, C.; Prasad, P. N. *Biomed. Microdevices* **2002**, *4*, 293–299.